An Analytic Circuit-Based Model for White and Flicker Phase Noise in *LC* Oscillators

Jayanta Mukherjee, Patrick Roblin, *Member, IEEE*, and Siraj Akhtar, *Member, IEEE*

***Abstract*—A general circuit-based model of *LC* oscillator phase noise applicable to both white noise and $1/f$ noise is presented. Using the Kurokawa theory, differential equations governing the relationship between amplitude and phase noise at the tank are derived and solved. Closed form equations are obtained for the IEEE oscillator phase noise for both white and $1/f$ noise. These solutions introduce new parameters which take into account the correlation between the amplitude noise and phase noise and link them to the oscillator circuit operating point. These relations are then used to obtain the final expression for Voltage noise power density across the output oscillator terminals assuming the noise can be modeled by stationary Gaussian processes. For white noise, general conditions under which the phase noise relaxes to closed-form Lorentzian spectra are derived for two practical limiting cases. Further, the buffer noise in oscillators is examined. The forward contribution of the buffer to the white noise floor for large offset frequency is expressed in terms of the buffer noise parameters. The backward contribution of the buffer to the $1/\Delta f^2$ oscillator noise is also quantified. To model flicker noise, the Kurokawa theory is extended by modeling each $1/f$ noise perturbation in the oscillator as a small-signal dc perturbation of the oscillator operating point. A trap-level model of flicker noise is used for the analysis. Conditions under which the resulting flicker noise relaxes to an $1/\Delta f^3$ phase noise distribution are derived. The proposed model is then applied to a practical differential oscillator. A novel method of analysis, splitting the noise contribution of the various transistors into modes is introduced to calculate the Kurokawa noise parameters. The modes that contribute the most to white noise and flicker noise are identified. Further, the tail noise contribution is analyzed and shown to be mostly up-converted noise. The combined white and flicker noise model exhibits the presence of a number of corner frequencies whose values depend upon the relative strengths of the various noise components. The proposed model is compared with a popular harmonic balance simulator and a reasonable agreement is obtained in the respective range of validity of the simulator and theory. The analytical theory presented which relies on measurable circuit parameters provides valuable insight for oscillator performance optimization as is discussed in the paper.**

***Index Terms*—Correlation, flicker noise, Kurokawa, Lorentzian, noise floor, phase noise, traps, uncorrelated modes, white noise.**

I. Introduction

OSCILLATOR phase noise is an important design criterion in any communication system [1]. The reciprocal mixing of oscillator phase noise with signal noise in RF transceivers causes a number of undesirable effects like inter-channel interference, increased bit-error rate (BER) and synchronization problem in digital systems. With complex modulation schemes like orthogonal frequency-division multiplexing (OFDM), the requirement of spectral purity becomes ever more stringent. Hence, achieving good phase noise performance and the means to model it becomes important.

A significant amount of work has been done in the field of phase noise characterization. Early models like those of Leeson propose a linear time-invariant (LTI) model of phase noise [2], [3]. These models tend to depict a $1/\Delta f^2$ dependence of voltage-spectral density thereby implying infinite noise power near the harmonics [1]. These models provide some limited insight into noise analysis and oscillator design. These simplified models do not give us a complete understanding of the oscillator noise spectrum. In order to improve the performance of the models, some approaches incorporated a linear time variant model of noise [4], [5]. These models give us a better explanation of certain portions of the frequency spectrum (like the $1/\Delta f^3$ region of an oscillator spectrum arising from $1/f$ noise and the corner frequency between the $1/\Delta f^3$ and $1/\Delta f^2$ regions). However, these models rely on complex functions which are difficult to compute in practical oscillators. Also the correlation factor between amplitude and phase fluctuations is neglected.

In a detailed paper on oscillator noise [6], Kaertner resolves the oscillator response into phase and magnitude components. A differential equation was obtained for the phase error. A similar effort was made in [1] where the oscillator response is described in terms of a phase deviation and an additive component called orbital deviation. Both [6] and [1] obtained the correct Lorentzian spectrum for the power-spectral density (PSD) due to white noise. However, neither of these models is circuit focused, and limited insight is therefore provided to the circuit designer. In summary though considerable work has been done in the field of oscillator noise analysis, to our knowledge no theory provides a circuit based approach using simple easy-to-measure parameters to describe the phase noise.

In this paper, we first develop differential equations for the amplitude and phase deviations treating noise as a perturbation. The fact that an oscillator can be linearized about its operating point is very much a valid concept as has been demonstrated in numerous papers [7]. We rely on the Kurokawa theory [8] for this purpose. The advantage of this approach is that it gives us a circuit focus and thus enables us to incorporate the circuit based parameters into the phase noise equations. We shall provide a more rigorous treatment of noise due to both phase and amplitude deviations with due consideration for correlation existing between the two [9]. In addition, most models, while giving de-

Manuscript received April 17, 2006; revised September 27, 2006. This work was supported in part by a Texas Instruments Fellowship. This paper was recommended by Associate Editor B. C. Levy.

J. Mukherjee was with the Department of Electrical and Computer Engineering, Ohio State University, Columbus, OH 43210 USA. He is now with the Department of Electrical Engineering, Indian Institute of Technology, Mumbai 400076, India

P. Roblin is with the Department of Electrical and Computer Engineering, Ohio State University, Columbus, OH 43210 USA (e-mail: roblin@ece.osu.edu).

S. Akhtar is with the RFIC design group of Texas Instruments, Dallas TX 75243 USA.

Digital Object Identifier 10.1109/TCSI.2007.898673

scriptions of oscillator phase noise do not account for the circuit buffer noise. In this paper we show how the buffer noise can be incorporated in the noise model to account for the oscillator noise floor while also contributing in part to the colored oscillator noise spectrum.

While white noise can be easily represented both in time as well as frequency domains, $1/f$ noise is not so easy to characterize. The fact that this noise has a $1/f$ frequency dependence implies that at $f = 0$, the noise power is infinite. Many researchers [6], [10] have postulated stationary process models or piecewise-stationary models to simplify the phase noise derivations. In our approach we will start our analysis at a single device trap level and then extend it for all traps as shown in [11].

In oscillators, $1/f$ noise has a tendency to get up-converted and produce a $1/\Delta f^3$ noise spectrum. To analyze the impact of $1/f$ noise on the oscillator we note that since the $1/f$ noise process is significant only at very low frequencies, the perturbation it causes to oscillation is equivalent to the perturbation of the dc bias of the devices involved. As we shall see, this model will help us in obtaining an analytical solution. The methodology used will further, enable us to take into consideration, the correlation between the phase and amplitude deviations due to noise which has been neglected in previous work.

Finally, we combine the expressions for phase noise due to white noise, flicker noise and buffer noise in one single closed form analytical expression and compare the model so obtained with harmonic balance simulation results.

II. Nonlinear Perturbation Analysis of a Oscillator

Fig. 1 shows a negative resistance oscillator model. The basic oscillator has been divided into a linear frequency sensitive part (having admittance $Y_L(\omega)$) and a nonlinear or device part (which is both frequency and amplitude sensitive and has admittance given by $Y_{IN}(A,\omega)$). In a conventional *LC* oscillator, the linear part usually represents the tank. For all derivations henceforth we shall consider the tank to be a parallel RLC circuit. In steady state, in the absence of noise and other perturbing signals, the operating point (A_0, ω_0) is given by

$$Y_L(\omega_0) + Y_{IN}(A_0, \omega_0) = 0.$$

$i_N(t)$ represents an equivalent noise source which arises due to noise sources in both the linear and the nonlinear parts of the oscillator circuit and which will be extracted in the example shown later. It can be shown (Appendix I) that the phase ϕ and amplitude deviation $\delta A (A = A_0 + \delta A)$ obey the following Langevin equations:

$$A_0 \beta \delta A(t) + \frac{d\delta A(t)}{dt} |Y_T'|^2 = i_{N1}(t) B_T' + i_{N2}(t) G_T' \quad (1)$$

$$A_0 \left[\alpha \delta A(t) + |Y_T'|^2 \frac{d\phi(t)}{dt} \right] = i_{N1}(t) G_T' - i_{N2}(t) B_T' \quad (2)$$

when the oscillator is linearized about its operating point voltage amplitude (A_0) and frequency (ω_0) [8], where the correlation factor α and stability factor β are given by

$$\alpha = G_T'(\omega_0) G_{IN}'(A_0, \omega_0) + B_T'(\omega_0) B_{IN}'(A_0, \omega_0)$$
$$\beta = B_T'(\omega_0) G_{IN}'(A_0, \omega_0) - G_T'(\omega_0) B_{IN}'(A_0, \omega_0)$$

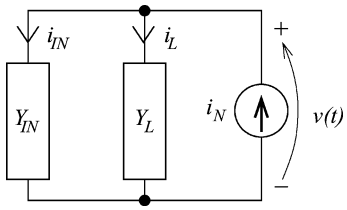

Fig. 1. Admittance model of an oscillator.

where i_{N1} and i_{N2} are obtained from i_N in Fig. 1 using

$$i_{N1}(t) = \frac{2}{T} \int_{t-T}^{t} i_N(t) \cos[\omega t + \phi(t)]\, dt \quad (3)$$

$$i_{N2}(t) = \frac{2}{T} \int_{t-T}^{t} i_N(t) \sin[\omega t + \phi(t)]\, dt. \quad (4)$$

Note that the processes δA and ϕ are similar to Ornstein–Uhlenbech processes [13] except that they are correlated. The term α accounts for the correlation between ϕ and δA (i.e., if $\alpha = 0$ there is no correlation). The terms $Y_T'(\omega_0)$ and $Y_{IN}'(A_0, \omega_0)$ which represent the variation of the admittances with perturbations, are given by

$$Y_T' = G_T'(\omega_0) + jB_T'(\omega_0) = \left.\frac{\partial Y_L}{\partial \omega}\right|_{\omega_0} + \left.\frac{\partial Y_{IN}}{\partial \omega}\right|_{A_0,\omega_0} \quad (5)$$

$$Y_{IN}' = G_{IN}'(A_0, \omega_0) + jB_{IN}'(A_0, \omega_0) = \left.\frac{\partial Y_{IN}}{\partial \delta A}\right|_{A_0,\omega_0}. \quad (6)$$

This is a more general treatment than in [8] which uses a frequency independent $Y_{IN}(A_0)$. If the voltage across the tank is given by

$$v(t) = A(t) \cos[\omega_0 t + \phi(t)] + \text{small harmonics}$$

then the autocorrelation of the voltage for stationary Gaussian noise processes is given by (see derivation in Appendix II)

$$R_V(\tau) = \frac{1}{2} \left[A_0^2 + R_{\delta A}(\tau) \right] \cos(\omega_0 \tau) \exp\left[R_\phi(\tau) - R_\phi(0) \right]. \quad (7)$$

$R_{\delta A}(\tau)$ and $R_\phi(\tau)$ represent the autocorrelation functions of the amplitude deviation δA and the phase ϕ, respectively. As is verified in Appendix III, $\delta A(t)$ and $\phi(t)$ are stationary processes for the noise processes considered in this paper under the assumption that the oscillator is on for a long enough time.

The first term in (7) which is proportional to A_0^2 is the phase modulation (PM) noise. The second term involving $R_{\delta A}(\tau)$ is the amplitude modulation (AM) noise term. Equation (7) is derived neglecting a third contribution arising from the correlation between phase and amplitude noises. This is justified as the PM noise will be verified below to be dominant over AM noise so that it can be assumed to be dominant as well over this third contribution.

We shall first consider white noise sources. Following Kurokawa [8], we have the following spectral densities:

$$S_{i_N}(f) = |e|^2, \quad S_{i_{N1}}(f) = S_{i_{N2}}(f) = 2|e|^2.$$

As is shown in Appendix III the expressions for $R_{\delta A}(\tau)$ and $R_\phi(\tau)$ are derived from the Langevin equations (1) and (2) to be given by

$$R_{\delta A}(\tau) = \frac{|e|^2}{A_0\beta}\exp(-\eta|\tau|)$$

$$R_\phi(\tau) = R_\phi(0) - \frac{|e|^2}{A_0^2\left|Y_T'(\omega_0)\right|^2}\left(1+\frac{\alpha^2}{\beta^2}\right)|\tau| - \frac{\alpha^2|e|^2}{\beta^3 A_0^3}\left[\exp(-\eta|\tau|)-1\right]$$

where we introduce the frequency η

$$\eta = \frac{A_0\beta}{|Y_T'(\omega_0)|^2}.$$

The autocorrelation function for the tank voltage is then

$$R_V(\tau) = \frac{1}{2}\left[A_0^2 + \frac{|e|^2}{A_0\beta}\exp(-\eta|\tau|)\right]\cos(\omega_0\tau) \times \exp\left[-\frac{|e|^2}{A_0^2\left|Y_T'(\omega_0)\right|^2}\left(1+\frac{\alpha^2}{\beta^2}\right)|\tau|\left(e^{-\eta|\tau|}-1\right)\right].$$

According to the Wiener–Khintchin theorem, the PSD of the voltage across the tank can now be obtained by taking the Fourier transform of $R_V(\tau)$

$$S_V(\omega) = \mathcal{F}\{R_V(\tau)\}.$$

Note that S_V is directly observable on a spectrum analyzer. $S_\phi(\omega)$ which is derived in Appendix III is the IEEE definition of phase noise [12] and requires a phase detector. For $\alpha = 0$ (no correlation) a closed form solution under the form of a Lorentzian (defined below) is obtained for S_V. No exact analytic solution is available for the Fourier transform of $R_V(\tau)$ when we account for the correlation between the amplitude and phase (α nonzero). However, an approximate analytical Lorentzian solution can be obtained for two practical limit conditions

$$S_{V,\mathrm{ssb}}(\omega) = \underbrace{A_0^2\left[\frac{m_1}{m_1^2+(\omega-\omega_0)^2}\right]}_{\text{PM Noise}} + \underbrace{c\left[\frac{m_1+\eta}{(m_1+\eta)^2+(\omega-\omega_0)^2}\right]}_{\text{AM Noise}} \quad (8)$$

where $S_{V,\mathrm{ssb}}(\omega)$ is the single side band (ssb) voltage-spectral density. In (8), we use $c = |e|^2/(A_0\beta)$ and define m_1 as

$$m_1 = \begin{cases} m_{01}, & \text{for } \Delta\omega \gg \eta \text{ or for } \alpha = 0 \text{ and all } \omega \\ m_{01}\left[1+\left(\frac{\alpha}{\beta}\right)^2\right], & \text{for } \eta \gg m_{01} \text{ and } \Delta\omega < \eta \end{cases}$$

$$\text{with } m_{01} = \frac{|e|^2}{A_0^2\left|Y_T'(\omega_0)\right|^2}.$$

The asymptotic result for $\Delta\omega > \eta$ is derived in Appendix VI using the stationary phase approximation. If η is very large the second approximation involving the correlation factor $(\alpha/\beta)^2$ is the relevant choice.

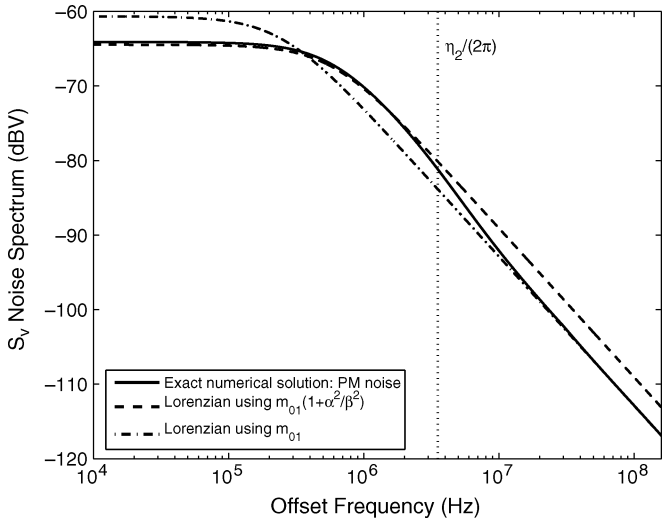

Fig. 2. Comparison of PM voltage noise spectrum with various Lorentzian approximations.

For intermediate value of η the Fourier transform of $R_V(\tau)$ can readily be calculated numerically. This is illustrated in Fig. 2 for $\eta/(2\pi) = 3.5$ MHz. As is shown in Fig. 2 $S_{V,\mathrm{ssb}}(\omega)$ is seen to relax for $\Delta\omega \gg \eta$ to the limiting Lorentzian with $\alpha = 0$. The voltage noise spectrum is no longer strictly a Lorentzian, and an inflexion point is introduced in the PM voltage noise density at the frequency $f_{2B} = \eta/(2\pi)$.

The expressions of S_V obtained for $\alpha = 0$ (no correlation) are consistent with other published works [1], [6]. A Lorentzian spectrum ensures that the total power of the oscillator remains finite. A $1/\Delta f^2$ spectrum of noise-spectral density for all frequencies on the other hand implies infinite oscillator power. Note that for large values of $\Delta\omega = \omega - \omega_0$ compared to m_1, the spectrum can be approximated as

$$S_{V,\mathrm{ssb}}(\omega) \simeq \frac{A_0^2 m_1}{\Delta\omega^2} + \frac{c(m_1+\eta)}{\Delta\omega^2}.$$

Integrating the phase noise over frequency it can be shown that

$$\int_{-\infty}^{\infty} S_V(\omega)df = \int_0^{\infty} S_{V,\mathrm{ssb}}(\omega)df = \frac{A_0^2+c}{2}$$

which is the same as the power of a noiseless oscillator if AM white noise is neglected ($c = 0$).

Fig. 3 compares the AM, PM, and (AM + PM) white noise component of $S_{V,\mathrm{ssb}}$ for a differential oscillator (introduced in Section V). On a logarithmic graph the approximate PM/AM Lorentzian spectra have corner frequencies given by $m_1/(2\pi) \simeq 0.6$ MHz and $(m_1+\eta)/(2\pi) \simeq 4.2$ MHz respectively. Since A_0^2 (PM noise) exceeds c (AM noise) (by 20 dB in Fig. 3) $m_1/(2\pi)$ is the corner frequency of the total (AM + PM) white noise spectrum.

The inflexion point at η observed in the PM noise spectrum is not easily observable in the total (AM+PM) noise spectrum due to the AM noise contribution. Agreement of the theory with the circuit simulator is verified to be within 0.6 dB at high offset frequencies ($\Delta\omega \gg m_1$) for the circuit considered.

Both m_1 and $m_1+\eta$ are proportional to $1/|Y_T'(\omega_0)|^2$. For a parallel tank, $|Y_T'(\omega_0)| \simeq 2C$ and is proportional to the tank

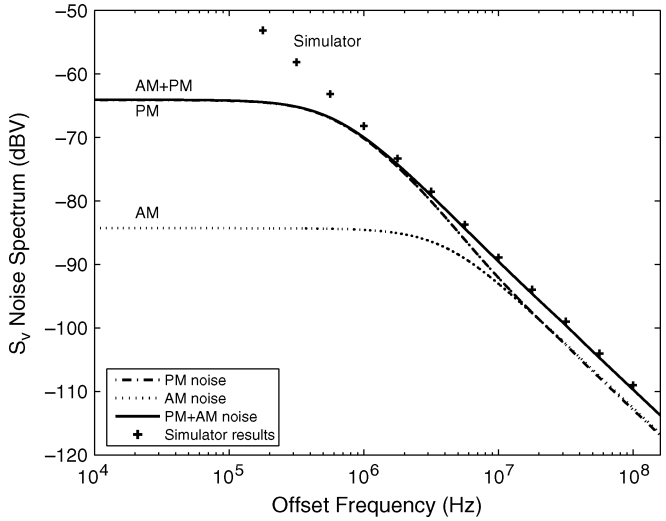

Fig. 3. Comparison of AM and PM white noise spectrum in a differential oscillator.

Q. This shows that at large offset frequencies $S_V(\omega)$ is proportional to $1/Q^2$, thus agreeing with Leeson's model. However the equation derived above presents the voltage noise in terms of easily measurable parameters $Y'_T(\omega_0)$ and $Y'_{IN}(A_0,\omega_0)$ in conventional harmonic balance simulation of oscillators.

The presence of the additional terms (α/β) in m_1 provides greater accuracy in the expression for the Voltage noise density. The ratio α/β has to be as low as possible for reducing phase noise

$$\frac{\alpha}{\beta}=\frac{[G'_T\ \ B'_T]\cdot[G'_{IN}\ \ B'_{IN}]}{[G'_T\ \ B'_T]\times[G'_{IN}\ \ B'_{IN}]}=\frac{|Y'_T|\,|Y'_{IN}|\cos\theta}{|Y'_T|\,|Y'_{IN}|\sin\theta}=\cot\theta$$

where θ is the angle between the complex vector Y'_T and Y'_{IN}. It results that when θ is 90° the noise correlation is minimized: $\alpha/\beta=0$. When θ is 0° the noise correlation is maximized: $\alpha/\beta=\infty$. This well known result was first inferred by Kurokawa [8] from the inspection of $S_\phi(\omega)$. One of the contributions of the present work for white noise is to introduce the correlation factor $\alpha/\beta=\cot\theta$ and to quantify the impact of the correlation on the overall phase noise spectra $S_V(\omega)$ of the oscillator. In the circuit considered, the correlation term is verified in Fig. 2 to bring a shift on the order of ±3.8 dB for frequencies below $\eta/(2\pi)$.

Kurokawa [8] provided a graphical interpretation of the correlation factor. In the limit where $Y'_T=Y'_L$, (active devices contributing minimally to the tank Q-factor), θ is the angle at the oscillator operating point (ω_0,A_0) between the locus of the device admittance line $Y_{IN}(A,\omega_0)$ as a function of A and the locus of the circuit admittance line $Y_L(\omega)$ as function of ω. Therefore, in the limit where $Y'_T=Y'_L$ holds, the oscillator noise is respectively maximized or minimized when the circuit and device admittances lines are tangent or perpendicular to one another.

For an ideal high Q parallel tank $(G'_T=G'_L=0)$ we have, $\cot\theta=B'_{IN}(A_0,\omega_0)/G'_{IN}(A_0,\omega_0)$. In other words, to make the ratio small the variation of device conductance and susceptance with respect to amplitude should be very high and low respectively. This is typically the case for active devices operating below f_T. In Section V, we will show how the white noise theory can be applied to a differential oscillator.

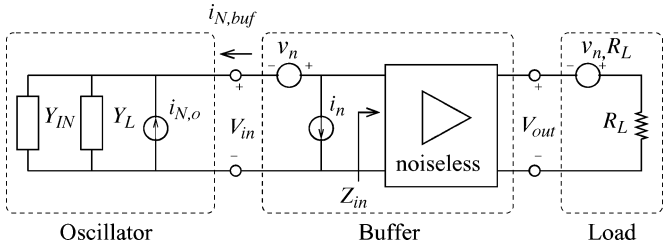

Fig. 4. Circuit for buffer noise modeling.

III. Buffer Noise

Most oscillator circuits have some kind of 2-port buffers to stabilize the load impedance. This can range from a simple pad attenuator to a differential output buffer stage as in the circuit to be considered in Section V. The impact of a 2-port buffer on the oscillator is usually not discussed in detail in the literature. Also most simulators neglect the presence of a noise floor introduced by the buffer in the output and shows the noise decreasing infinitely with increasing offset frequency.

Consider the noisy 2-port equivalent circuit for the buffer circuit shown in Fig. 4 which features the usual input-referred noise current i_n and noise voltage v_n.

Using the results given in Appendix V the Norton equivalent noise current $i_{N,\mathrm{buff}}$ injected by the buffer network in the oscillator circuit is given by

$$i_{N,\mathrm{buff}}=i_n+\frac{v_n}{Z_{\mathrm{in}}}+Y_o v_{n,R_L}$$

with

$$Z_{\mathrm{in}}=\frac{1}{Y_{\mathrm{in}}}=z_{11}-\frac{z_{12}z_{21}}{R_L+z_{22}}$$

and

$$Y_o=\frac{1}{z_{21}}\left(\frac{z_{11}}{Z_{\mathrm{in}}}-1\right).$$

It results that the noise current power density $\overline{i^2_{N,\mathrm{buff}}}$ injected by the buffer in the oscillator is

$$\overline{i^2_{N,\mathrm{buff}}}=\overline{i^2_u}+|Y_{\mathrm{in}}+Y_C|^2\overline{v^2_n}+|Y_o|^2\overline{v^2_{n,R_L}}$$

where Y_C is the correlation admittance $i_c=Y_C v_n$. In these expressions, i_u is the uncorrelated component and i_c the correlated noise component of the total buffer noise current $i_n=i_u+i_c$. The load noise $\overline{v^2_{n,R_L}}$ and the buffer noises can themselves be expressed as

$$\overline{v^2_n}=4k_BTR_n,\quad \overline{v^2_{n,R_L}}=4k_BTR_L\quad\text{and}\quad \overline{i^2_u}=4k_BTG_u.$$

Thus, an additional component $\overline{i^2_{N,\mathrm{buff}}}$ gets added to $\overline{i^2_{N,o}}=|e|^2$ in the total $\overline{i^2_N}$ and the definition of m_1 changes to

$$m_1=\frac{\left(|e|^2+|i_{N,\mathrm{buff}}|^2\right)}{A_0^2\,|Y'_T(\omega_0)|^2}\left(1+\frac{\alpha^2}{\beta^2}\right).$$

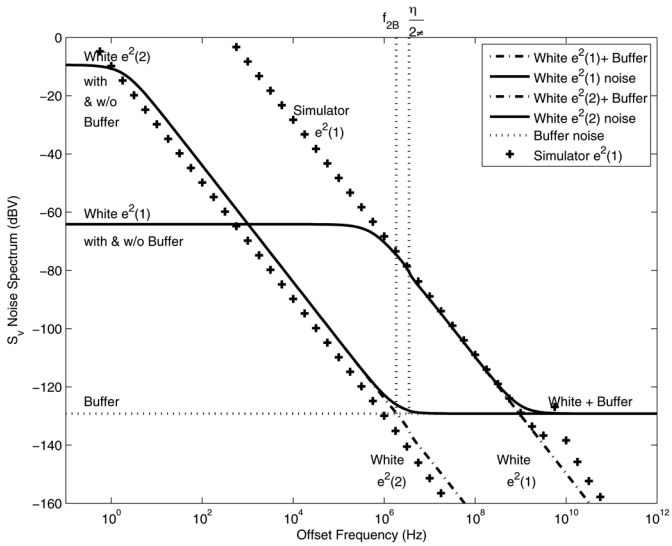

Fig. 5. Impact of buffer white noise on the voltage-spectral density $S_{V_{\rm out}}/|A_v|^2$ of a differential oscillator.

The equivalent voltage noise source v_n appearing at the input contributes directly to the input-referred noise floor. The total noise at the output of the buffer including the buffer noise is then

$$\begin{aligned} S_{V_{\rm out}}(\omega) &= |A_v|^2 \left(S_{V,\rm ssb}(\omega) + \overline{v_{N,\rm buff}^2} \right) \\ &= |A_v|^2 \left(S_{V,\rm ssb}(\omega) + \overline{v_n^2} + \overline{v_{n,R_L}^2} \left| \frac{z_{11}}{z_{21}} \right|^2 \right) \end{aligned}$$

where A_v is the voltage gain provided by the buffer

$$A_v = \frac{z_{21} R_L}{Z_{11}(R_L + z_{22}) - z_{12} z_{21}}.$$

$\overline{v_n^2}$ (i.e., R_n) is usually the leading term contributing to the noise floor in high-Q LC oscillators. The impact of the noise floor is illustrated in Fig. 5 for a buffer noise floor of -130 dBV with two different white noise strengths of $e^2(1) = 8.5 \times 10^{-18}$ A^2/Hz (unusually strong white noise) and $e^2(2) = 2.8 \times 10^{-23}$ A^2/Hz (normal weaker white noise). The corner frequency between white noise and noise floor is given by

$$f_{2F} = \frac{1}{2} \sqrt{\frac{A_0^2 m_1}{v_{N,\rm buff}^2}}.$$

Note that f_{2B} for white noise of usual strength $e^2(2)$ is on the order $\eta/(2\pi)$ and therefore m_1 should indeed be used instead of m_{01} in the frequency range ($\Delta f < f_{2B}$) where white noise dominates. Note also that of the 6-dB offset between model (plain line) and simulator ($+$) results for $e^2(2)$, 4 dB are due to the new $(1 + \cot^2 \theta)$ correlation factor.

IV. Extending the Model to Flicker Noise

In order to extend the Kurokawa analysis to $1/f$ noise we can study the effect of a variation of the dc current $i_N = I_0 + \delta i_N$ in any oscillator component, upon the active admittance Y_{IN}. Using a linearization scheme similar to the one we employed in the white noise case we get (defining $0 = (A_0, \omega_0, I_0)$)

$$\begin{aligned} Y_{IN}(A, \omega, i_N) = Y_{IN}(A_0, \omega_0, I_0) &+ \left. \frac{\partial Y_{IN}}{\partial A} \right|_0 \delta A \\ &+ \left. \frac{\partial Y_{IN}}{\partial \omega} \right|_0 \delta \omega + \left. \frac{\partial Y_{IN}}{\partial i_N} \right|_0 \delta i_N. \quad (9) \end{aligned}$$

With the additional derivative term at the end, the master equations become

$$\frac{|Y_T'(\omega_0)|^2}{A_0} \frac{d\delta A(t)}{dt} + \beta \delta A(t) = B \delta i_N(t) \quad (10)$$

$$|Y_T'(\omega_0)|^2 \frac{d\phi(t)}{dt} + \alpha \delta A(t) = -A \delta i_N(t) \quad (11)$$

where the new constant A and B are given by

$$\begin{aligned} A &= G_T'(\omega_0) B_{IN}^{i_N\prime}(0) - B_T'(\omega_0) G_{IN}^{i_N\prime}(0) \\ B &= G_T'(\omega_0) G_{IN}^{i_N\prime}(0) + B_T'(\omega_0) B_{IN}^{i_N\prime}(0) \end{aligned}$$

with

$$Y_{IN}^{i_N\prime}(0) = G_{IN}^{i_N\prime}(0) + j B_{IN}^{i_N\prime}(0) = \left. \frac{\partial Y_{IN}}{\partial i_N} \right|_{A_0, \omega_0, I_0}.$$

$\delta i_N(t)$ will be defined by its power density $S_{\delta i_N, 1/f}(\omega) = S/|\omega|$ in the next section.

A. Solving the Differential Equations and Obtaining the Expression for the Voltage Noise Density

We use the autocorrelation function of the charge trapping model of the flicker noise to find the final noise voltage density as shown in [17]. The goal is to obtain a stationary model of flicker noise. We first assume the autocorrelation function is wide-sense stationary (WSS) and equal to (Ornstein–Uhlenbeck assumption [13])

$$R_{\delta i_N}(\tau) = k e^{-\lambda |\tau|}. \quad (12)$$

Taking the Fourier transform of $R_{\delta i_N}(\tau)$ gives the noise density as

$$S_{\delta i_N}(\omega) = \frac{2\lambda k}{\omega^2 + \lambda^2}. \quad (13)$$

This autocorrelation corresponds to a random telegraph noise which has a Lorentzian distribution. A superposition of many of these processes with time constants $\tau_{\rm trap}(y) = 1/\lambda = \tau_S \exp(\rho y)$ which are spatially varying with position y in the oxide (MOS) or wide-bandgap region (HFET), will result in a noise process with a $1/f$ distribution

$$\begin{aligned} S_{\delta i_N, 1/f}(\omega) &= \int_0^{d_{max}} S_{\delta i_N}(\omega) dy = \frac{1}{\rho} \int_{\lambda_0}^{\lambda_1} S_{\delta i_N}(\omega) \frac{(-d\lambda)}{\lambda} \\ &= \frac{2k}{\rho\omega} \left[\tan^{-1}\left(\frac{\lambda_0}{\omega} \right) - \tan^{-1}\left(\frac{\lambda_1}{\omega} \right) \right] \\ &\simeq \frac{k\pi}{\rho\omega} = \frac{S}{\omega} \quad \text{for } \lambda_1 < \omega < \lambda_0 \end{aligned}$$

where $\lambda_0 = 1/\tau_S \simeq \infty$, $\lambda_1 = 1/\tau_{\rm trap}(d_{max}) \simeq 0$ and $S = k\pi/\rho$. The superposition is valid since we assume the different traps behave independently.

We take the Fourier transform of (10) and (11) and express the RHS of each equation in a simplified form.

$$\frac{|Y_T'(\omega_0)|^2}{A_0} j\omega\delta A(\omega) + \beta\delta A(\omega) = B\delta i_N(\omega) \quad (14)$$

$$|Y_T'(\omega_0)|^2 j\omega\phi(\omega) + \alpha\delta A(\omega) = -A\delta i_N(\omega). \quad (15)$$

From (14) we obtain

$$S_{\delta A,1\rm trap}(\omega) = \frac{2B^2\lambda k}{(\lambda^2+\omega^2)\left(\beta^2 + \frac{\omega^2|Y_T'(\omega_0)|^4}{A_0^2}\right)}. \quad (16)$$

Note that we have used the expression for $S_{\delta i_N}(\omega)$ from (13) to calculate $S_{\delta A,1\rm trap}(\omega)$. From (15), we get

$$S_{\phi,1\rm trap}(\omega) = \frac{2\lambda k}{\omega^2|Y_T'(\omega_0)|^4(\lambda^2+\omega^2)} \times \left[\frac{\frac{\omega^2|Y_T'(\omega_0)|^4A^2}{A_0^2} + (\beta A+\alpha B)^2}{\frac{|Y_T'(\omega_0)|^4\omega^2}{A_0^2} + \beta^2}\right]. \quad (17)$$

The expression above can be simplified as

$$S_{\phi,1\rm trap}(\omega) = K_\phi\left[\frac{\omega^2+k_1}{\omega^2(\omega^2+k_2)(\omega^2+k_3)}\right] \quad (18)$$

with, $K_\phi = 2\lambda k\kappa^2$, $\kappa = A/|Y_T'(\omega_0)|^2$, $k_1 = A_0^2(\beta A + \alpha B)^2/(A^2|Y_T'(\omega_0)|^4)$, $k_2 = \lambda^2$ and $k_3 = A_0^2\beta^2/|Y_T'(\omega_0)|^4 = \eta^2$. Decomposing (18) into partial fractions we obtain

$$S_{\phi,1\rm trap}(\omega) = K_\phi\left[\frac{n_1}{\omega^2} - \frac{n_2}{k_2+\omega^2} - \frac{n_3}{k_3+\omega^2}\right] \quad (19)$$

where $n_1 = k_1/(k_2k_3)$, $n_2 = (k_1-k_2)/k_2(k_3-k_2)$, and $n_3 = (k_1-k_3)/k_3(k_2-k_3)$. From which we obtain

$$R_{\phi,1\rm trap}(\tau) = \mathcal{F}^{-1}\left[S_{\phi,1\rm trap}(\omega)\right] = -\frac{K_\phi}{2}\left[n_1|\tau| + \frac{n_2}{\lambda}e^{-\lambda|\tau|} + \frac{n_3}{\eta}e^{-\eta|\tau|}\right] \quad (20)$$

with for a single trap $R_{\phi,1\rm trap}(0) = \sigma^2 = K_\phi[-(n_2/2\lambda) - (n_3/2\eta)]$. Equation (16) can be expanded into partial fractions as

$$S_{\delta A,1\rm trap}(\omega) = K_{\delta A}\left[\frac{1}{(\omega^2+k_3)(\omega^2+k_2)}\right] = \frac{K_{\delta A}}{k_2-k_3}\left[\frac{1}{\omega^2+k_3} - \frac{1}{\omega^2+k_2}\right] \quad (21)$$

where $K_{\delta A} = 2B^2\lambda k A_0^2/|Y_T'(\omega_0)|^4$ and $k_2 = \lambda^2$. Taking the inverse Fourier transform of $S_{\delta A,1\rm trap}(\omega)$, we obtain $R_{\delta A,1\rm trap}(\tau)$

$$R_{\delta A,1\rm trap}(\tau) = \frac{K_{\delta A}}{2(k_2-k_3)}\left[\frac{e^{-\eta|\tau|}}{\eta} - \frac{e^{-\lambda|\tau|}}{\lambda}\right]. \quad (22)$$

The resulting $R_{V,1\rm trap}$ is given by

$$\begin{aligned}R_{V,1\rm trap}(\tau) &= \frac{A_0^2 + R_{\delta A,1\rm trap}(\tau)}{2}\cos(\omega_0\tau) \times \exp[R_{\phi,1\rm trap} - \sigma^2] \\ &= \frac{A_0^2 + R_{\delta A,1\rm trap}(\tau)}{2}\cos(\omega_0\tau) \times \exp\left[-\frac{K_\phi}{2}\left(n_1|\tau| + \frac{n_2}{\lambda}\left(e^{-\lambda|\tau|}-1\right) + \frac{n_3}{\eta}\left(e^{-\eta|\tau|}-1\right)\right)\right] \\ &= \frac{A_0^2}{2}\cos(\omega_0\tau) \times \exp\left[-\frac{K_\phi}{2}\left(n_1|\tau| + \frac{n_2}{\lambda}\left(e^{-\lambda|\tau|}-1\right) + \frac{n_3}{\eta}\left(e^{-\eta|\tau|}-1\right)\right)\right] \\ &\quad + \frac{K_{\delta A}}{4\eta(k_2-k_3)}\cos(\omega_0\tau) \times \exp\left[-\frac{K_\phi}{2}\left(n_1|\tau| + \frac{n_2}{\lambda}\left(e^{-\lambda|\tau|}-1\right) + \frac{n_3}{\eta}\left(e^{-\eta|\tau|}-1\right)\right) - \eta|\tau|\right] \\ &\quad - \frac{K_{\delta A}}{4\lambda(k_2-k_3)}\cos(\omega_0\tau) \times \exp\left[-\frac{K_\phi}{2}\left(n_1|\tau| + \frac{n_2}{\lambda}\left(e^{-\lambda|\tau|}-1\right) + \frac{n_3}{\eta}\left(e^{-\eta|\tau|}-1\right)\right) - \lambda|\tau|\right]. \end{aligned} \quad (23)$$

As shown in Appendix VII using the method of stationary phase the Fourier transform of $R_{\phi,1\rm trap}(\tau)$ for large offset frequencies $\Delta\omega = \omega - \omega_0$ is given by (using a ssb representation)

$$\begin{aligned}S_{V_{1trap},\rm ssb}(\omega) &= \frac{A_0^2K_\phi}{2}\left[\frac{n_2k_2}{\Delta\omega^2(k_2+\Delta\omega^2)} + \frac{n_3k_3}{\Delta\omega^2(k_3+\Delta\omega^3)}\right] + \frac{K_{\delta A}}{2(k_2-k_3)}\left[\frac{1}{k_3+\Delta\omega^2} - \frac{1}{k_2+\Delta\omega^2}\right] \\ &= \frac{A_0^2K_\phi(k_1+\Delta\omega^2)}{2\Delta\omega^2(k_3+\Delta\omega^2)(\lambda^2+\Delta\omega^2)} + \frac{K_{\delta A}}{2(k_3+\Delta\omega^2)(\lambda^2+\Delta\omega^2)}.\end{aligned}$$

This expression gives the noise-spectral density at large offset frequency for a single trap (i.e., for a particular value of λ). Note that Appendix VII can be applied to derive the PM component because the terms q_1, q_2, and q_3 which can be identified for a single trap in $R_{V,1\rm trap}$ verify $q_1+q_2+q_3 = 0$ thus satisfying the required property $\sum_k q_k = 0$.

The IEEE definition of phase noise for $1/f$ noise $S_{\phi,1/f}$ is obtained with the summation of the single-trap phase noise over

all traps

$$S_{\phi,1/f}(\omega)=\frac{1}{\rho}\int_{\lambda_0}^{\lambda_1} S_{\phi,1\mathrm{trap}}(\omega)\frac{(-d\lambda)}{\lambda}\simeq\frac{S\kappa^2(\omega^2+k_1)}{\omega^2(\omega^2+k_3)}$$
$$=\frac{2k\kappa^2(\omega^2+k_1)}{\rho\omega^2(\omega^2+k_3)}\left[\tan^{-1}\left(\frac{\lambda_0}{\omega}\right)-\tan^{-1}\left(\frac{\lambda_1}{\omega}\right)\right].$$

Similarly, before we calculate $R_{V,1/f}$ and $S_{V,1/f}$ we need to evaluate the autocorrelation $R_{\phi,1/f}(\tau)$ and $R_{\delta A,1/f}(\tau)$ by summing over all traps. These integrations yield closed form expressions for $R_{\delta A,1/f}(\tau)$ and $R_{\phi,1/f}(\tau)$ [see (24)]. These analytic solutions are quite useful for verification purposes and we shall use them to obtain the exact voltage noise density $S_{V,1/f}(\omega)$ by calculating numerically the Fourier transform of $R_{V,1/f}(\tau)$

$$\begin{aligned}R_{\phi,1/f}(\tau)&=\frac{1}{\rho}\int_{\lambda_0}^{\lambda_1} R_{\phi,1\mathrm{trap}}(\tau)\frac{(-d\lambda)}{\lambda}\\&=\frac{K'_\phi}{2\rho}\left[\frac{k_1-k_3}{2k_3^2}e^{-\eta\tau}\left\{\ln\left|\frac{\lambda_1-\eta}{\lambda_0-\eta}\right|-\ln\left|\frac{\lambda_1+\eta}{\lambda_0+\eta}\right|\right\}\right.\\&\quad+\frac{k_1-k_3}{2k_3^2}\left\{e^{-\eta|\tau|}[\mathrm{Ei}[(\eta-\lambda_0)|\tau|]-\mathrm{Ei}[(\eta-\lambda_1)|\tau|]]\right.\\&\quad+e^{\eta|\tau|}[\mathrm{Ei}[-(\lambda_0+\eta)|\tau|]-\mathrm{Ei}[-(\lambda_1+\eta)|\tau|]]\\&\quad\left.+2\mathrm{Ei}(-\lambda_1|\tau|)-2\mathrm{Ei}(-\lambda_0|\tau|)\right\}\\&\quad+\frac{k_1}{k_3}\left\{\frac{e^{-\lambda_0|\tau|}}{2\lambda_0^2}-\frac{e^{-\lambda_1|\tau|}}{2\lambda_1^2}\right.\\&\quad+\left(\frac{1}{\lambda_0}-\frac{e^{-\lambda_0|\tau|}}{2\lambda_0}-\frac{1}{\lambda_1}+\frac{e^{-\lambda_1|\tau|}}{2\lambda_1}\right)|\tau|\\&\quad\left.\left.+(\mathrm{Ei}(-\lambda_1|\tau|)-\mathrm{Ei}(-\lambda_0|\tau|))\frac{|\tau|^2}{2}\right\}\right]. \quad (24)\end{aligned}$$

An analytic expression for $S_{V,1/f}$ valid for large offset frequencies can also be obtained using the method of stationary phase. This is due to the fact that the key assumption made in Appendix VII namely $\sum_k q_k = 0$ still holds when summing (integrating) over all the traps. It results by applying the results of Appendix VII that for large enough offset frequencies the voltage noise density of flicker noise is simply obtained by averaging over all values of λ the expression obtained for the voltage noise density of a single trap contribution

$$\begin{aligned}S_{V,1/f,\mathrm{ssb}}(\omega)&=\frac{1}{\rho}\int_{\lambda_0}^{\lambda_1} S_{V1\mathrm{trap}}(\omega)\frac{(-d\lambda)}{\lambda}\\&=\left\{\frac{A_0^2K'_\phi}{2\rho\Delta\omega^2}\frac{k_1+\Delta\omega^2}{k_3+\Delta\omega^2}+\frac{K'_{\delta A}}{2\rho}\frac{1}{k_3+\Delta\omega^2}\right\}\\&\quad\times\int_{\lambda_0}^{\lambda_1}\frac{1}{\lambda^2+\Delta\omega^2}(-d\lambda)\\&=\left\{\frac{A_0^2K'_\phi}{2\rho\Delta\omega^2}\frac{k_1+\Delta\omega^2}{k_3+\Delta\omega^2}+\frac{K'_{\delta A}}{2\rho}\frac{1}{k_3+\Delta\omega^2}\right\}\\&\quad\times\frac{1}{\Delta\omega}\left[\tan^{-1}\left(\frac{\lambda_0}{\Delta\omega}\right)-\tan^{-1}\left(\frac{\lambda_1}{\Delta\omega}\right)\right]\end{aligned}$$

where $K'_\phi = K_\phi/\lambda$ and $K'_{\delta A} = K_{\delta A}/\lambda$. In the limit of $\lambda_0 = \infty$ and $\lambda_1 = 0$ this reduces to

$$S_{V,1/f,\mathrm{ssb}}(\omega)=\frac{A_0^2S\kappa^2}{2}\left[\frac{k_1+\Delta\omega^2}{\Delta\omega^3(\eta^2+\Delta\omega^2)}\right]+\frac{A_0^2SB^2}{2\,|Y_T'(\omega_0)|^4}\frac{1}{\Delta\omega(\eta^2+\Delta\omega^2)}. \quad (25)$$

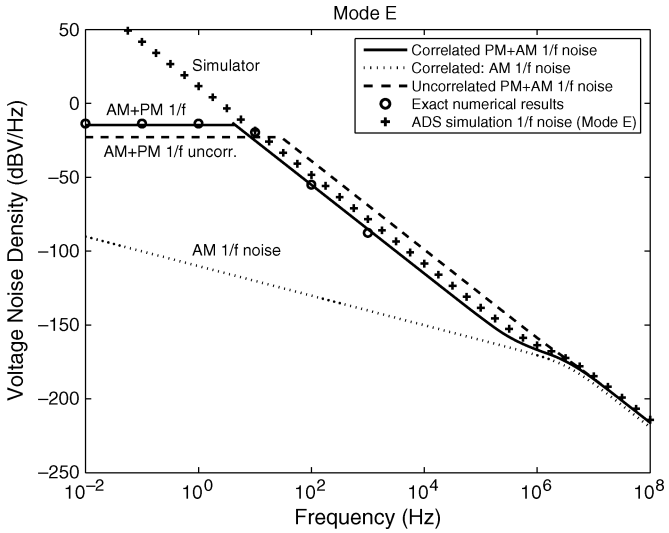

Fig. 6. Comparison of analytic expression for $\mathrm{AM}+\mathrm{PM}$ and AM with exact numerical solution and simulator results.

Fig. 6 shows the analytic expressions obtained for $\mathrm{AM}+\mathrm{PM}$ $1/f$ noise (plain line) and for AM $1/f$ noise (dotted line). The test circuit used is the differential oscillator to be discussed in Section V. The voltage noise spectra reported are for $1/f$ noise originating in the tail transistor (Mode E). Also shown in Fig. 6 are the results obtained for $\mathrm{AM}+\mathrm{PM}$ $1/f$ noise (dashed line) for the uncorrelated case $(\alpha = 0)$. Clearly correlation can play an important role for mode E as it leads to a 30-dB decrease in noise in the $1/\Delta f^3$ region.

At low offset frequencies (here below 1 Hz) the stationary phase approximation fails as indicated by the exact numerical results (circles). A simple estimate of the ceiling voltage noise density $S_{V,1/f}(\mathrm{ceiling})$ and corner frequency $\Delta f_{1/f}(\mathrm{ceiling})$ can be obtained by enforcing power conservation and assuming a $1/\Delta f^3$ spectrum up to the corner frequency

$$S_{V,1/f}(\mathrm{ceiling})=0.6\times\frac{A_0^3}{\sqrt{F}}\ \text{with}\ F=\frac{A_0^2S\kappa^2k_1}{2\eta^2}$$
$$\Delta f_{1/f}(\mathrm{ceiling})=\frac{1}{2\pi}\left(\frac{F}{S_{V,1/f}(\mathrm{ceiling})}\right)^{\frac{1}{3}}.$$

Agreement with circuit simulation is only of 7 dB for mode E. Better agreement will be obtained for other dominant $1/f$

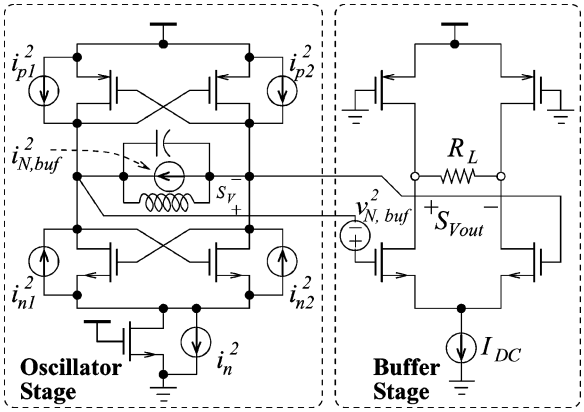

Fig. 7. Differential oscillator with buffer stage.

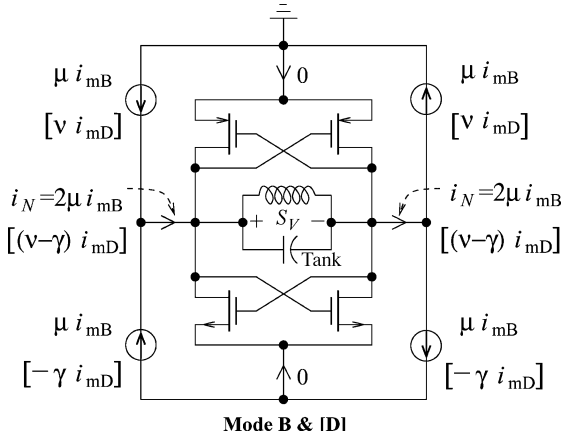

Fig. 8. Modes B and D for a differential oscillator. These two modes inject a noise current i_N directly across the tank.

modes (A and C) in Section V when correlation brings a weaker correction.

V. Comparison of Proposed Model With a Practical Differential Oscillator

Let us consider the differential oscillator shown in Fig. 7. The tank is selected to form the linear part of the oscillator while the remaining of the circuit forms the nonlinear part.

A. Mode Analysis of the Oscillator

The Kurokawa analysis is typically used in harmonic balance simulators for calculating the oscillator operating point (A_0, ω_0) using $\Gamma_L(\omega_0) \times \Gamma_{IN}(A_0, \omega_0) = 1$. Consequently the various nonlinear device and linear tank admittances are readily available for applying the circuit based noise model presented above. However a method for calculating the equivalent noise source appearing across the tank is needed to apply the noise theory developed in the previous sections for the white noise analysis. The methodology introduced for this purpose will also facilitate the $1/f$ analysis by reducing the number of independent modes (noise sources) considered from 5 to 3.

Fig. 7 shows the schematic of a simple differential oscillator having four 'core' transistors. $\overline{i_{p1}^2}$ and $\overline{i_{p2}^2}$ represent the noise produced by pMOS transistors while $\overline{i_{n1}^2}$ and $\overline{i_{n2}^2}$ represent the noise produced by the nMOS transistors. Note that for white noise the gate and drain noise currents (see for example [14])

$$\overline{i_{p/n,d}^2} = 4k_BT\gamma_{\rm MOS}g_m \quad \text{and} \quad \overline{i_{p/n,g}^2} = 4k_BT\delta_{\rm MOS}g_g$$

of opposite nMOS and pMOS transistors (n1 and n2 or p1 and n2) appear in parallel due to the circuit topology such that we have for example $\overline{i_{p1}^2} = \overline{i_{p1,d}^2} + \overline{i_{p2,g}^2}$. For the rest of the analysis we define $\overline{|i_{n1}|^2} = \overline{|i_{n2}|^2} = a$ and $\overline{|i_{p1}|^2} = \overline{|i_{p2}|^2} = b$. For $1/f$ noise we similarly have $a = S_a/|\omega| = (S_{n1,d} + S_{n2,g})/|\omega|$ and $b = S_b/|\omega| = (S_{p1,d} + S_{p2,g})/|\omega|$.

The first step for the mode analysis is to split the instantaneous noise currents of the four transistors into uncorrelated unit mode currents.

Let N be the matrix which converts the transistor noise currents into these uncorrelated mode currents, i.e.,

$$i_{\rm mode} = N i_{\rm trans}$$

where $i_{\rm mode}$ and $i_{\rm trans}$ are given by

$$i_{\rm mode} = \begin{bmatrix} i_{m_A} \\ i_{m_B} \\ i_{m_C} \\ i_{m_D} \end{bmatrix} \quad \text{and} \quad i_{\rm trans} = \begin{bmatrix} i_{p_1} \\ i_{p_2} \\ i_{n_1} \\ i_{n_2} \end{bmatrix}. \tag{26}$$

Since $i_{\rm mode}$ consists of uncorrelated mode currents having unit power density, we have

$$\overline{|i_{\rm mode}|^2} = i_{\rm mode} \cdot i_{\rm mode}^T = N i_{\rm trans} \cdot i_{\rm trans}^T N^T = \begin{bmatrix} 1 & 0 & 0 & 0 \\ 0 & 1 & 0 & 0 \\ 0 & 0 & 1 & 0 \\ 0 & 0 & 0 & 1 \end{bmatrix}.$$

It can be shown that a possible matrix N is given by

$$N = \begin{bmatrix} \frac{1}{a_n} & \frac{1}{a_n} & \frac{1}{b_n} & \frac{1}{b_n} \\ \frac{1}{a_n} & -\frac{1}{a_n} & \frac{1}{b_n} & -\frac{1}{b_n} \\ c & c & -c & -c \\ c & -c & -c & c \end{bmatrix} \tag{27}$$

with $a_n = a\sqrt{(2/a) + (2/b)}$, $b_n = b\sqrt{(2/a) + (2/b)}$, $c = 1/\sqrt{2(a+b)}$. Reversely we have $i_{\rm trans} = N^{-1} i_{\rm mode}$ with N^{-1} given by

$$N^{-1} = \begin{bmatrix} \mu & \mu & \nu & \nu \\ \mu & -\mu & \nu & -\nu \\ \mu & \mu & -\gamma & -\gamma \\ \mu & -\mu & -\gamma & \gamma \end{bmatrix}$$

where, μ, ν and γ are given by

$$\mu = \sqrt{\frac{ab}{2(a+b)}}, \quad \nu = \frac{a}{\sqrt{2(a+b)}}, \quad \gamma = \frac{b}{\sqrt{2(a+b)}}.$$

We have now expressed $i_{\rm trans}$ in terms of a certain number of uncorrelated unity strength mode currents. Fig. 8 shows the schematic representation of modes B and D.

As seen from Table I when the noise currents are substituted by a single tone perturbation, each mode contributes differently to the noise current injected across the tank by either up-conversion or direct transfer. For modes A and C the largest contribution to the current i_N across the tank at $f_0 + \Delta f$ is coming

TABLE I
RESPONSE IN DECIBEL VOLTS OF THE TANK VOLTAGE AT $f_0 + \Delta f$ TO A SINGLE TONE EXCITATION INJECTED IN THE CIRCUIT WITH 1-kHz AND (1-MHz) OFFSET Δf FROM VARIOUS HARMONICS nf_0

Input Offset	Mode A (dBV)	Mode B (dBV)	Mode C (dBV)	Mode D (dBV)	Mode E (dBV)
Δf	-96 (-96)	-296 (-293)	-84 (-84)	-293 (-303)	-101 (-101)
f_0+Δf	-300 (-294)	-95 (-95)	-700 (-700)	-92 (-92)	-700 (-700)
$2f_0$+Δf	-700 (-700)	-700 (-700)	-700 (-700)	-700 (-700)	-700 (-700)
$3f_0$+Δf	-700 (-700)	-700 (-700)	-700 (-700)	-700 (-700)	-700 (-700)

from the *up-conversion* of the input currents $i_{mA/C}$ at Δf. For modes B and D the largest contributions to the current i_N injected across the tank at $f_0 + \Delta f$ is coming from the *transfer* of the input currents at $i_{mB/D}$ at $f_0 + \Delta f$. It results that modes B and D are most significant for white noise and modes A and C are most significant for $1/f$ noise. The tail current leakage of each of the individual mode noises is verified to be usually insignificant in a differential oscillator (the tail current source acts as an open for modes A to D).

As shown in Fig. 8, the resultant currents across the tank for modes B and D are 2μ and $(\nu - \gamma)$ respectively. The effect of individual modes can be accounted by adding their relative contributions to R_ϕ and $R_{\delta A}$, respectively, i.e., for white noise,

$$R_\phi = R_{\phi_B} + R_{\phi_D}$$
$$R_{\delta A} = R_{\delta A_B} + R_{\delta A_D}.$$

The resulting voltage noise density S_V obtained will be the same as the one we previously reported in Section II if $|e|^2$ is replaced now by

$$|e|^2 = |e_B|^2 + |e_D|^2.$$

If we consider the total i_N flowing across the tank due to modes B and D, we get

$$S_{i_N}(\omega) = 4\mu^2 + (\nu - \gamma)^2 = \frac{a+b}{2} = |e|^2.$$

For white noise this result is the same as the noise current density across the tank given in [16]. For $1/f$ noise we need to calculate $G_{IN}^{i_N\prime}(A_0, \omega_0, I_0)$ and $B_{IN}^{i_N\prime}(A_0, \omega_0, I_0)$ for mode A and C. One can select δ_{i_N} to be 2 μ and ν for mode A and C, respectively. For mode C, if we calculate $G_{IN}^{i_N\prime}(A_0, \omega_0, I_0)$ and $B_{IN}^{i_N\prime}(A_0, \omega_0, I_0)$ using $\delta_{i_N} = \nu m_C = 1$ nA for the two top current sources in Fig. 8, then the two bottom current sources are given by $\gamma m_C = \gamma/\nu\ \delta_{i_N} = a/b\ \delta_{i_N} = a/b \times 1$ nA. Note that for $1/f$ noise $a/b = S_a/S_b$ is frequency independent.

Note that our model neglects the frequency dependence of the oscillator on the perturbating current δ_{i_N}. As can be verified in Fig. 9, this is a reasonable assumption up to 1-MHz offset for the differential oscillator considered in this paper.

B. Impact of Tail Noise

For completeness we need to consider the impact of tail noise on the overall voltage noise density. We refer to the tail noise analysis as Mode E. However unlike the previous modes, the noise current of the tail current is directly the mode current. Table I shows the effect of a single frequency tone with 1-kHz and 1-MHz offset relative to dc, ω_0, and $2\omega_0$, respectively. The results are similar to those obtained for cases A and C. In other words, the up-converted noise dominates over the transferred noise.

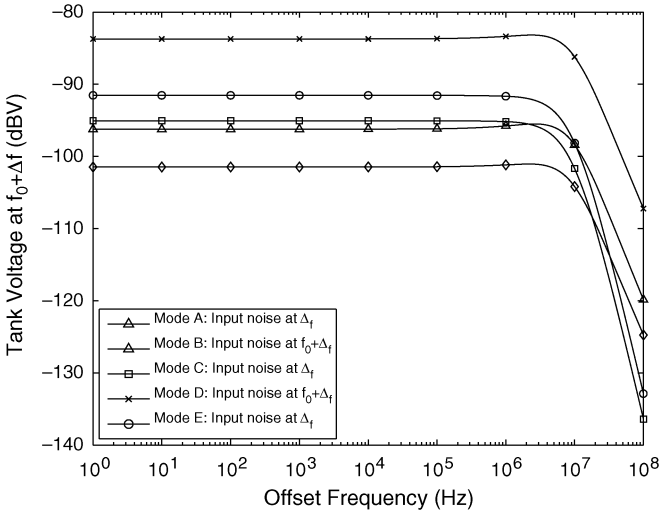

Fig. 9. Impact of the tank voltage at $f_0 + \Delta f$ of a 1-nA perturbation current at various offsets Δf for Mode A through E.

C. Obtaining the Circuit Parameters $Y_T(\omega_0)$ and $Y_{IN}(A_0, \omega_0)$

The operating point $(f_0, A_0) \simeq (2.466\ \text{GHz}, 1.15\ \text{V}|)$ for the oscillator was obtained using conventional harmonic balance simulation. An accuracy of 0.1 Hz and 8 μV was achieved. The convergence accuracy of the voltage and current was set to 1×10^{-15} A and 1×10^{-15} V, respectively, in the harmonic balance simulations. Up to eight harmonics were used in the harmonic balance simulations.

By changing A about the operating point, $Y'_{IN}(A_0, \omega_0)$ can be obtained. Similarly by changing ω about the operating point, $\partial Y_{IN}/\partial\omega$ can be computed, which in turn leads us to $Y'_T(\omega_0)$. A quadratic convergence of the derivatives calculated was observed for shrinking derivative intervals. A least square fit was further used to remove any residual numerical noise. The maximum error bound (e.g., $|\Delta Y'_{IN}(A_0, \omega_0)/Y'_{IN}(A_0, \omega_0)|$) in the derivatives calculated was of $2 \times 10^{-6}\%$ in relative magnitude. These derivatives can also be obtained from measurements of the device and tank impedances [19].

D. Comparing the Various $1/f$ Modes

In our simulations we used for the $1/f$ noise sources $S_a = 4 \times 10^{-18}$ A^2 and $S_b = 1 \times 10^{-18}$ A^2 which are within the range specified for a standard CMOS process. For mode E we used $S_E = 0.25 \times 10^{-18}$ A^2. The various $1/f$ modes are compared in Fig. 10. Mode A is found to be dominant for the circuit simulated and noise parameters selected. In the presence of mismatches within the nMOS and pMOS transistor pairs mode E could play a more prevalent role. Fig. 11 compares next the model and simulator results when all $1/f$ modes are accounted for. Agreement with noise simulation with our microwave circuit simulator is reasonable within the range of validity of the simulation.

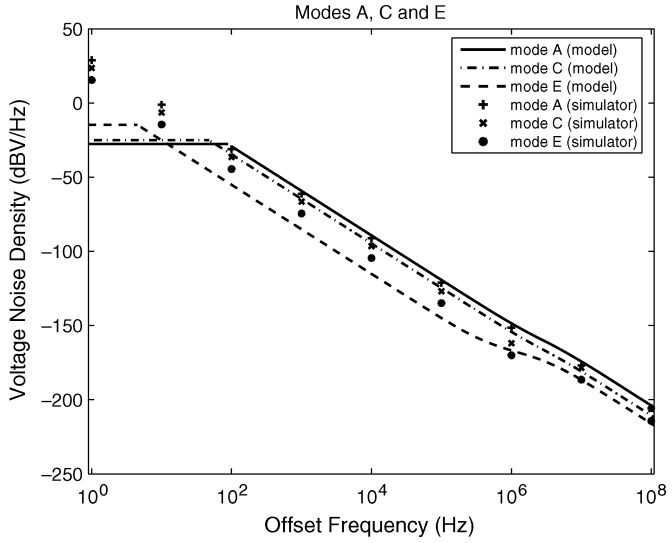

Fig. 10. Comparison of $1/f$ modes A, C, and E.

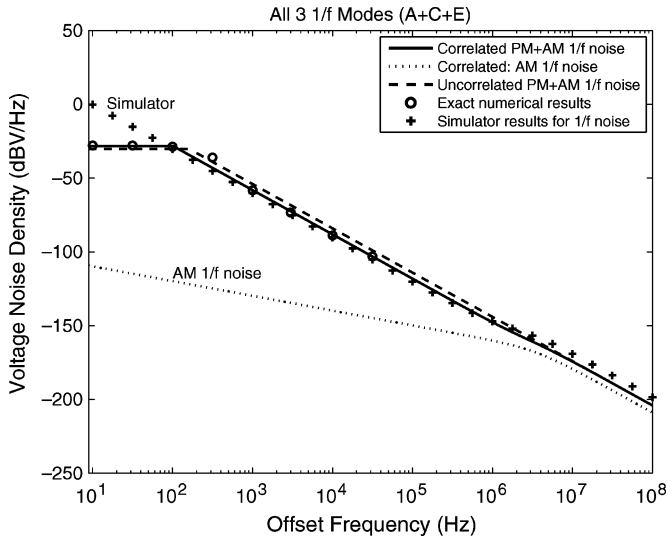

Fig. 11. Comparison of model and simulator results for the AM and $\mathrm{AM}+\mathrm{PM}$ $1/f$ noise for all modes summed (A+C+E).

VI. Combined White and $1/f$ Noise

Here, we consider both white and flicker noise together. As we have already seen when studying white noise and flicker noise to properly evaluate the combined effect of multiple independent noise processes on the oscillator output voltage-spectral density we must first sum their respective phase and amplitude autocorrelations

$$R_{\phi,\mathrm{tot}}(\tau) = R_{\phi,1/f}(\tau) + R_{\phi,\mathrm{white}}(\tau)$$
$$R_{\delta A,\mathrm{tot}}(\tau) = R_{\delta A,1/f}(\tau) + R_{\delta A,\mathrm{white}}(\tau)$$

before calculating the voltage-spectral density $S_{V,\mathrm{tot}}$. The commonly used approach which consists of summing the voltage-spectral density of white noise and flicker noise

$$S_{V,\mathrm{tot}}(\tau) = S_{V,1/f}(\tau) + S_{V,\mathrm{white}}(\tau)$$

is an approximation. As we shall demonstrate below, the validity of this approximation will depend on the relative strengths of the $1/f$ noise and white noise processes.

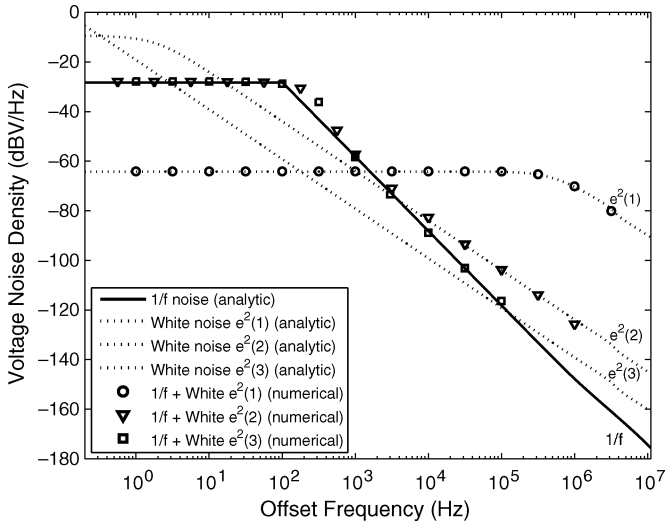

Fig. 12. Comparison of the Voltage noise densities when white and flicker noise summed (circle, square, star) with flicker noise (plain line) and white noise (dashed line, dashed dotted line, dotted line) for three different white noise levels.

Consider the two corner frequencies $\Delta f_{\mathrm{white}}(\mathrm{ceiling}) = m_1/(2\pi)$ and $\Delta f_{1/f}(\mathrm{ceiling})$ at which the voltage-spectral density reaches its ceiling value when respectively considering white noise or flicker noise separately.

When the corner frequency $\Delta f_{\mathrm{white}}(\mathrm{ceiling})$ of white noise is *larger* than the corner frequency $\Delta f_{1/f}(\mathrm{ceiling})$ of flicker noise then *no* $1/\Delta f^3$ region will be present in the $S_{V,\mathrm{tot}}(\omega)$ noise spectrum since the ceiling dictated by power conservation has already been reached. This is numerically verified to take place in Fig. 12 in the presence of a strong white noise $e^2(1) = 8.5 \times 10^{-18}$ A^2/Hz when the total voltage density (circles) follows the white noise Lorentzian spectra and not the flicker noise spectra. Clearly in this strong white noise case the usual summation of the voltage-spectral density of white noise and flicker noise would lead to incorrect noise spectra prediction. Although the impact of $1/f$ noise would not be detectable in the $S_{V,\mathrm{tot}}(\omega)$ voltage noise spectrum, it will be detected in $S_{\phi,\mathrm{tot}}(\omega)$ and $R_\phi(\tau)$ which can be measured using a phase detector.

On the other hand if the corner frequency $\Delta f_{\mathrm{white}}(\mathrm{ceiling})$ is smaller than the corner frequency $\Delta f_{1/f}(\mathrm{ceiling})$ then the $1/\Delta f^3$ region will be observed in the $S_{V,\mathrm{tot}}(\omega)$ voltage noise spectrum. This is the case in Fig. 12 in the presence of the weaker white noise $e^2(2) = e^2(1)/(3 \times 10^5)$ and $e^2(3) = e^2(1)/10^7$ when the total (white + flicker) voltage densities (triangle) follow first the $1/\Delta f^3$ flicker noise spectra at low offset frequencies before switching at high offset frequencies to the $1/\Delta f^2$ noise spectra. In such a case the corner frequency between the $1/\Delta f^2$ and $1/\Delta f^3$ regions is given by (assuming mode A dominating)

$$\Delta f_{23} = \frac{1}{2\pi}\frac{k_{1,A}}{\eta^2}\frac{S_A\kappa_A^2}{2m_1}.$$

The usual summation of the voltage-spectral density of white noise and flicker noise is then an excellent approximation. In summary the simple rules described above for combining noise

processes permit us to predict the total noise spectrum from the analytic models without resorting to numerical analysis.

VII. Conclusion

In this paper, we have presented an extension of the Kurokawa theory of oscillators to more accurately model white noise and to apply it to flicker noise. The proposed model takes into account correlations existing between the amplitude and phase voltage noises at the tank (embodied by the α and β factors). Approximate analytic expressions were derived for the voltage noise spectra. These analytic expressions were verified to hold for a wide range of frequencies using both numerical analysis relying on the exact solution $R_\phi(\tau)$ and by comparison with an harmonic balance simulator for a differential oscillator. For this purpose a mode theory of noise was developed to facilitate the calculation of the various Kurokawa noise parameters needed. This mode theory also provides valuable insights in the various noise up-conversion/transfer processes. The impact of the buffer on the oscillator was also accounted for. Finally rules for combining various uncorrelated noise (e.g., white and flicker) were presented and verified with numerical simulation.

The theory presented here is certainly not without its own limitations. The circuit was assumed not to be afflicted by strong memory effects (very low frequency dc to RF frequency dispersion) besides traps. This facilitated the obtaining of an analytic solution for $1/f$ noise. Our derivation focused principally on PM phase noise which is the dominant term compared to the AM noise which was also derived. There exists however the possibility for a third type of combined AM-PM noise for strongly correlated amplitude and phase noises. This noise would be suppressed if the buffer acts an amplitude limiter. [4]. Note that the expressions obtained for the IEEE phase noise definition $S_\phi(\omega)$ remain themselves unaffected by this approximation.

This circuit based-approach used also provides increased insights in the noise processes. Specifically for white noise the analytic model points towards the need to effectively reduce the amplitude and phase noise correlation ($\cot\theta = \alpha/\beta$). According to the analytic models derived in this work, Leeson's formula for large offset frequencies should be updated to be (assuming $G'_T \simeq 0$, $\Delta f_{\text{white}}(\text{ceiling}) < \Delta f_{1/f}(\text{ceiling})$, $\Delta\omega_{23} < \eta$ and $\Delta\omega_{23} < \sqrt{k_1}$)

$$\begin{aligned} L &= \frac{S_{V,\text{tot,ssb}}}{\frac{1}{2}A_0^2} \\ &= \frac{1}{P_S}\left[v_n^2 G_L + \frac{|e|^2\left(1+\cot^2\theta\right)}{(2Q)^2}\frac{\omega_0^2}{\Delta\omega^2}\right] \\ &\quad + \frac{S\left(G_{IN}^{i_N\prime} - \cot\theta B_{IN}^{i_N\prime}\right)^2}{(2QG_L)^2}\frac{\omega_0^2}{\Delta\omega^3} \\ &\text{for} \quad \Delta f(\text{ceiling}) < \Delta f < \eta/(2\pi) \end{aligned}$$

with $P_S = (1/2)A_0^2 G_L$, the resonator $Q = \omega_0 \text{Im}\{\text{Y}'_\text{T}\}/(2\text{G}_\text{L}) \simeq \omega_0 \text{C}/\text{G}_\text{L}$ and using for example $G_L = \text{Re}\{\text{Y}_\text{L}\}$ for the resonator + buffer conductance. Although more accurate formulas are given within the paper this simplified expression should be useful to circuit designers to identify device and circuit parameters which are critical for phase noise optimization.

Appendix I
Derivations of Equations (1) and (2)

Let us consider an admittance model of an oscillator as shown in Fig. 1. The circuit behaves as an open at resonance and a short for the harmonics. The voltage $v(t)$ is then

$$\begin{aligned} v(t) &= \text{Re}\left[A(t)e^{j(\omega t+\phi(t))}\right] + \text{small harmonics} \\ \text{with} \quad \omega_i &= \omega + \frac{d\phi}{dt} - j\frac{1}{A(t)}\frac{dA(t)}{dt} = \omega + \delta\omega. \end{aligned} \tag{28}$$

The current $i_{IN}(t)$ in the nonlinear part can be expressed as

$$i_{IN}(t) = \text{Re}\left[A(t)e^{j(\omega t+\phi(t))}Y_{IN}(A_0, w_i)\right] + \text{large harmonics}. \tag{29}$$

Similarly, the current i_L flowing through the linear part is

$$i_L(t) = \text{Re}\left[A(t)e^{j(\omega t+\phi(t))}Y_L\right] + \text{large harmonics}. \tag{30}$$

Hence the current $i_N = i_L + i_{IN}$ can be given by

$$\begin{aligned} i_N = \text{Re}\Big\{A(t)e^{j(\omega t+\phi(t))}\left[Y_L(\omega_i) + Y_{IN}(A_0,\omega_i)\right]\Big\} \\ + \text{large harmonics}. \end{aligned} \tag{31}$$

We shall assume that the quantities $d\phi/dt$ and $(1/A)(dA/dt)$ are much smaller than ω. Performing a Taylor series expansion in both Y_L and Y_{IN}, multiplying then both sides of (31) by $\cos(\omega t + \phi(t))$ and $-\sin(\omega t + \phi(t))$ and finally integrating each of those equations in time over one time period of oscillation we obtain the following relations

$$\begin{aligned} i_{N1} &= \frac{2}{T}\int_{t-T}^{t} i_N \cos\left(\omega t + \phi(t)\right) dt \\ &= A(t)\Bigg(G_L(\omega) + G_{IN}(A,\omega) \\ &\qquad + G'_T(\omega)\frac{d\phi}{dt} + \frac{B'_T}{A}\frac{dA}{dt}\Bigg) \end{aligned} \tag{32}$$

$$\begin{aligned} -i_{N2} &= -\frac{2}{T}\int_{t-T}^{t} i_N \sin\left(\omega t + \phi(t)\right) dt \\ &= A(t)\Bigg(B_L(\omega) + B_{IN}(A,\omega) \\ &\qquad + B'_T(\omega)\frac{d\phi}{dt} - \frac{G'_T}{A}\frac{dA}{dt}\Bigg). \end{aligned} \tag{33}$$

Note that we have used the steady state ($dA/dt = d\phi/dt = 0$, $\omega_i = \omega$ and $i_N = 0$) conditions

$$G_L(\omega_0) + G_{IN}(A_0,\omega_0) = 0 \tag{34}$$

$$B_L(\omega_0) + B_{IN}(A_0,\omega_0) = 0. \tag{35}$$

Equations (32) and (33) can be further simplified by noting that for perturbative δA we can write

$$G_L(\omega)+G_{IN}(A,\omega)=\frac{\partial G_{IN}(A_0,\omega_0)}{\partial A}\delta A$$
$$B_L(\omega)+B_{IN}(A,\omega)=\frac{\partial B_{IN}(A_0,\omega_0)}{\partial A}\delta A.$$

Hence (32) and (33) can be simplified as

$$\frac{i_{N1}}{A_0}=\frac{\partial G_{IN}(A_0,\omega_0)}{\partial A}\delta A+G'_T(\omega_0)\frac{d\phi}{dt}+\frac{B'_T(\omega_0)}{A_0}\frac{d\delta A}{dt}$$
$$-\frac{i_{N2}}{A_0}=\frac{\partial B_{IN}(A_0,\omega_0)}{\partial A}\delta A+B'_T(\omega_0)\frac{d\phi}{dt}-\frac{G'_T(\omega_0)}{A_0}\frac{d\delta A}{dt}.$$

The above 2 equations can be rewritten as

$$\frac{d\delta A}{dt}\left|Y'_T(\omega_0)\right|^2+A_0\beta\delta A=i_{N1}B'_T(\omega_0)+i_{N2}G'_T(\omega_0)$$
$$A_0\left(\left|Y'_T(\omega_0)\right|^2\frac{d\phi}{dt}+\alpha\delta A\right)=i_{N1}G'_T(\omega_0)-i_{N2}B'_T(\omega_0)$$

which are the required master equations. These equations are the same as those derived by Kurokawa [8] except that we have in addition accounted for the frequency dependence of the $Y_{IN}(A,\omega)$ beside its amplitude dependence via the new coefficient Y'_T (see (5)) replacing Y'_L.

Appendix II
Derivations of $R_V(\tau)$

The autocorrelation function of the oscillation at times t and $t+\tau$ is (as shown in [15])

$$\begin{aligned}R_V(t,t+\tau)&=\left(A_0^2+R_{\delta A}\right)\cos\left[\omega_0 t+\phi(t)\right]\\&\quad\times\cos\left[\omega_0(t+\tau)+\phi(t+\tau)\right]\\&=\frac{1}{2}\left[A_0^2+R_{\delta A}(\tau)\right]\cos\omega_0\tau\\&\quad\times\cos\left[\phi(t+\tau)-\phi(t)\right].\end{aligned}\tag{36}$$

This derivation assumes δA and ϕ are uncorrelated. This assumption is often justified on the basis that the buffer acts as a limiter which suppresses the δA fluctuation at its output. We will be able to keep track of δA in this work to monitor its contribution. If $\phi_1=\phi(t)$ and $\phi_2=\phi(t+\tau)$ are jointly normal with zero mean and $\sigma_1=\sigma_2=\sigma$, then

$$\begin{aligned}f\left(\phi(t),\phi(t+\tau);t,t+\tau\right)&=\frac{1}{2\pi\sigma^2\sqrt{1-r^2}}\\&\quad\times\exp\left[-\frac{1}{2(1-r^2)\sigma^2}\left(\phi_1^2-2R_\phi\phi_1\phi_2+\phi_2^2\right)\right]\end{aligned}$$

where $R_\phi(\tau)=\sigma^2 r(\tau)=E[\phi(t+\tau)\phi(t)]$ with r the correlation coefficient.

Taking, $\Delta=\phi_1-\phi_2$ and $\Sigma=\phi_1+\phi_2$, we get

$$\begin{aligned}E\left[\cos(\phi_1-\phi_2)\right]&=\frac{1}{2\pi\sigma^2\sqrt{1-r^2}}\\&\quad\times\int_{-\infty}^{\infty}\int_{-\infty}^{\infty}\cos(\phi_2-\phi_1)\\&\quad\times\exp\left[\frac{\phi_1^2-2r\phi_1\phi_2+\phi_2^2}{2(1-r^2)\sigma^2}\right]d\phi_1 d\phi_2\\&=\frac{1}{4\pi\sigma^2\sqrt{1-r^2}}\sqrt{2\pi\sigma_\Sigma^2}\\&\quad\times\int_{-\infty}^{\infty}\cos(\Delta)\exp\left[\frac{-\Delta^2}{2\sigma_\Delta^2}\right]d\Delta\end{aligned}$$

with $2\sigma_\Sigma^2=4(1+r)\sigma^2$ and $2\sigma_\Delta^2=4(1-r)\sigma^2$. We get

$$E\left[\cos(\phi_1-\phi_2)\right]=\exp\left[-\frac{\sigma_\Delta^2}{2}\right]=\exp\left[R_\phi(\tau)-\sigma^2\right]$$

Hence from (36), we have using $\sigma^2=R_\phi(0)$

$$R_V(\tau)=\frac{1}{2}\left[A_0^2+R_{\delta A}(\tau)\right]\cos(\omega_0\tau)\exp\left[R_\phi(\tau)-R_\phi(0)\right].$$

Appendix III
Derivation of $R_\phi(\tau)$ and $R_{\delta A}(\tau)$

If we assume (1) and (2) hold for all time (oscillator on for a long time) and $i_{N1}(t)$ and $i_{N2}(t)$ are stationary processes then $A(t)$ and $\phi(t)$ are also themselves stationary [18]. Taking the Fourier transform of the (1) and (2), we get

$$\begin{aligned}&j\omega\frac{\delta A(\omega)}{A_0}\left|Y'_T\right|^2+\beta\delta A(\omega)\\&\quad=\frac{1}{A_0}\left[i_{N1}(\omega)B'_T+i_{N2}(\omega)G'_T\right]\end{aligned}\tag{37}$$

$$\begin{aligned}&j\omega\left|Y'_T\right|^2\phi(\omega)+\alpha\delta A(\omega)\\&\quad=\frac{1}{A_0}\left[i_{N1}(\omega)G'_T-i_{N2}(\omega)B'_T\right].\end{aligned}\tag{38}$$

From (37), we get the amplitude variation-spectral density

$$S_{\delta A}(\omega)=\frac{2\left|Y'_T(\omega_0)\right|^2|e|^2}{A_0^2\beta^2+\omega^2\left|Y'_T(\omega_0)\right|^4}$$

using $|i_{N1}(\omega)|^2=|i_{N2}(\omega)|^2=2|e|^2$ [8]. $R_{\delta A}(\tau)$ is then

$$R_{\delta A}(\tau)=\frac{|e|^2}{A_0\beta}\exp\left(-\frac{A_0\beta|\tau|}{\left|Y'_T(\omega_0)\right|^2}\right).\tag{39}$$

From (38), we get the following expression for $S_\phi^{(1)}$:

$$\begin{aligned}S_\phi^{(1)}(\omega)&=\frac{|e|^2}{\omega^2\left|Y'_T(\omega_0)\right|^4}\left[\frac{2\left|Y'_T(\omega_0)\right|^2}{A_0^2}+\alpha^2|\delta A|^2\right]\\&=\frac{2|e|^2}{A_0^2\left|Y'_T(\omega_0)\right|^2\omega^2}\left(1+\frac{\alpha^2}{\beta^2}\right)\\&\quad-\frac{\left|Y'_T(\omega_0)\right|^2}{\omega^2\left|Y'_T(\omega_0)\right|^4+A_0^2\beta^2}\times\frac{2|e|^2\alpha^2}{A_0^2\beta^2}.\end{aligned}$$

This result is in agreement with [20] for the uncorrelated δA and ϕ case ($\alpha/\beta = 0$). Note that the general solution of (38) is valid up to an arbitrary impulse

$$S_\phi(\omega) = S_\phi^{(1)}(\omega) + 2\pi\left(\sigma^2 + \frac{\alpha^2|e|^2}{\beta^3 A_0^3}\right)\delta(\omega). \quad (40)$$

The impulse weight is selected so as to satisfy the nonzero boundary condition of $R_\phi(0) = \sigma^2$. By taking the inverse Fourier transform of the (40) we obtain for the correlated case

$$R_\phi(\tau) = \sigma^2 - \frac{|e|^2}{A_0^2|Y_T'(\omega_0)|^2}\left(1+\frac{\alpha^2}{\beta^2}\right)|\tau| - \frac{\alpha^2|e|^2}{\beta^3 A_0^3}\left[\exp\left(-\frac{\beta A_0}{|Y_T'(\omega_0)|^2}|\tau|\right) - 1\right].$$

Here, we have used the relation $\alpha^2 + \beta^2 = |Y_{IN}'(A_0,\omega_0)|^2|Y_T'(\omega_0)|^2$. These results have been computed using the following inverse Fourier Transforms pairs

$$\mathcal{F}^{-1}\left[\frac{1}{\omega^2}\right] = -\frac{1}{2}|\tau| \text{ and } \mathcal{F}^{-1}\left[\frac{1}{\xi^2+\omega^2}\right] = \frac{1}{2\xi}\exp(-\xi|\tau|).$$

Appendix IV
Derivation of $S_V(\omega)$ for White Noise Case

Given the value derived for $R_\phi(\tau)$ and $R_{\delta A}$ we obtain

$$R_V(\tau) = \frac{1}{2}\left[A_0^2 + \frac{|e|^2}{A_0\beta}\exp(-\eta|\tau|)\right]\times\cos(\omega_0\tau) \times \exp\left[-\frac{|e|^2}{A_0^2|Y_T'(\omega_0)|^2}\left(1+\frac{\alpha^2}{\beta^2}\right)|\tau| - \frac{\alpha^2|e|^2}{\beta^3 A_0^3}\left(e^{-\eta|\tau|}-1\right)\right]$$

Now taking the Fourier transform of the above equation and proceeding along the method of stationary phase (see Appendix VI for the calculation of the Fourier transform of an exponential of an exponential), we obtain

$$S_{V,\text{ssb}}(\omega) = \underbrace{A_0^2\left[\frac{m_{01}}{m_{01}^2+(\omega-\omega_0)^2}\right]}_{\text{PM Noise}} + \underbrace{c\left[\frac{m_{01}+\eta}{(m_{01}+\eta)^2+(\omega-\omega_0)^2}\right]}_{\text{AM Noise}} \quad (41)$$

where $m_{01} = |e|^2/A_0^2|Y_T'(\omega_0)|^2$, $\eta = A_0\beta/|Y_T'(\omega_0)|^2$ and $c = |e|^2/A_0\beta$. Since $(\omega+\omega_0)^2$ is very high compared to m_1^2, those terms containing it in the denominator have been neglected.

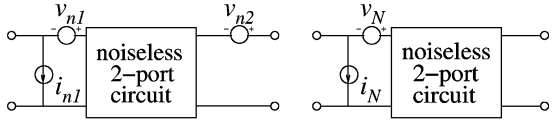

Fig. 13. Conventional noise model: (a) for a 2-port circuit loaded with an output noise source v_{n2} and (b) its equivalent input-referred representation.

Appendix V
Input Referred Load Noise

Consider the two circuits shown in Fig. 13. One readily verifies that the voltages v_N and i_N can be expressed in terms of i_{n1}, v_{n1} and v_{n2} using the following relation:

$$i_N = i_{n1} - \frac{v_{n2}}{z_{21}} \quad \text{and} \quad v_N = v_{n1} + \frac{z_{11}}{z_{21}}v_{n2}.$$

Appendix VI
Fourier Transform of $f(\tau)$ With Exponential of Exponential: White Noise Case

Let us consider $f(\tau)$ having a form as follows:

$$f(\tau) = \exp\left[-P\left(q_1|\tau| + \frac{q_2}{\eta}\left(e^{-\eta|\tau|}-1\right)\right)\right]$$

where $q_1 \neq q_2$. Taking the Fourier transform of $f(\tau)$ we get for $\mathcal{F}[f(\tau)]$ the result given in (42) at the bottom of the page.

$$\begin{aligned}
\mathcal{F}[f(\tau)] &= \int_{-\infty}^{\infty} f(\tau)e^{-j\omega\tau}d\tau = \int_{-\infty}^{\infty}\exp\left[-P\left(q_1|\tau| + \frac{q_2}{\eta}\left(e^{-\eta|\tau|}-1\right)\right) - j\omega\tau\right]d\tau \\
&= \int_{-\infty}^{0}\frac{\frac{d}{d\tau}\exp\left[-P\left(-q_1\tau + \frac{q_2}{\eta}(e^{\eta\tau}-1)\right) - j\omega\tau\right]d\tau}{P(q_1 - q_2e^{\eta\tau}) - j\omega} + \int_{0}^{\infty}\frac{\frac{d}{d\tau}\exp\left[-P\left(q_1\tau + \frac{q_2}{\eta}(e^{-\eta\tau}-1)\right) - j\omega\tau\right]d\tau}{-P(q_1 - q_2e^{-\eta\tau}) - j\omega} \\
&= \left[\frac{\exp\left(-P\left(-q_1\tau + \frac{q_2}{\eta}(e^{\eta\tau}-1)\right) - j\omega\tau\right)}{P(q_1 - q_2e^{\eta\tau}) - j\omega}\right]_{-\infty}^{0} + \int_{-\infty}^{0}\frac{(-P)q_2\eta e^{\eta\tau}\exp\left[-P\left(-q_1\tau + \frac{q_2}{\eta}(e^{\eta\tau}-1)\right) - j\omega\tau\right]}{[P(q_1 - q_2e^{\eta\tau}) - j\omega]^2} \\
&\quad + \left[\frac{\exp\left(-P\left(q_1\tau + \frac{q_2}{\eta}(e^{-\eta\tau}-1)\right) - j\omega\tau\right)}{-P(q_1 - q_2e^{-\eta\tau}) - j\omega}\right]_{0}^{\infty} + \int_{0}^{\infty}\frac{(-P)q_2\eta e^{-\eta\tau}\exp\left[-P\left(q_1\tau + \frac{q_2}{\eta}(e^{-\eta\tau}-1)\right) - j\omega\tau\right]}{[-P(q_1 - q_2e^{-\eta\tau}) - j\omega]^2}
\end{aligned} \quad (42)$$

The terms within the integration sign can be neglected since they become negligible for higher frequencies (method of stationary phase). Hence, the final expressions become

$$\mathcal{F}[f(\tau)] \approx \frac{2P(q_1-q_2)}{P^2(q_1-q_2)^2+\omega^2} \quad \text{for } \omega > \eta. \tag{43}$$

For our purpose, $q_1 = m_{01}(1+(\alpha^2/\beta^2))$, $q_2 = (\alpha^2/\beta^2)m_{01}$, and $m_{01} = |e|^2/[A_0^2|Y_T'(\omega_0)|^2]$. As a result

$$F(\omega) = \mathcal{F}[f(\tau)] = \frac{2m_{01}}{m_{01}^2+\omega^2}. \tag{44}$$

For white noise, we need the following Fourier transform:

$$\begin{aligned} S'_{\text{white}}(\omega) &= \mathcal{F}[f(\tau)\cos(\omega_0\tau)] \\ &= \frac{1}{2}F(\omega-\omega_0) + \frac{1}{2}F(\omega+\omega_0) \\ &= \frac{m_{01}}{m_{01}^2+(\omega-\omega_0)^2} + \frac{m_{01}}{m_{01}^2+(\omega+\omega_0)^2} \end{aligned} \tag{45}$$

At RF frequencies $(\omega+\omega_0)^2$ becomes very large and hence the second term becomes quite small compared to the first and can be neglected in an ssb representation

$$S'_{\text{white,ssb}}(\omega) \approx \frac{2m_{01}}{m_{01}^2+(\omega-\omega_0)^2} \quad (\omega > 0 \text{ only.})$$

Appendix VII
Fourier Transform of $f(\tau)$ With Exponential of Exponential: Flicker Noise Case

Consider a function $f(\tau)$ of the following form:

$$f(\tau) = \exp\left[-P\left(q_1|\tau| + \sum_{i=2}^{n}\frac{q_i}{\eta_i}\left(e^{-\eta_i|\tau|}-1\right)\right)\right]$$
$$\text{with} \quad \sum_{i=2}^{n} q_i = q_1 \quad \text{and} \quad P > 0. \tag{46}$$

We wish to calculate its Fourier transform shown in the equation at bottom of page.

Integrating by parts twice, we get for $F(\omega)$ the result shown in (47) at the bottom of the page. The terms within the integration sign will vanish in the limit $\omega \to \infty$ because they are rapidly varying functions of time (method of stationary phase). So $F(\omega)$ becomes

$$\begin{aligned} F(\omega) = &-P\sum_{i=2}^{n} q_i\eta_i\left(\frac{1}{(\eta_i-j\omega)(-j\omega)^2}\right. \\ &\left.-\frac{1}{(-\eta_i-j\omega)(-j\omega)^2}\right) \\ = &\frac{P}{\omega^2}\sum_{i=2}^{n}\frac{2q_i\eta_i^2}{\eta_i^2+\omega^2} \end{aligned}$$

$$\begin{aligned} F(\omega) = \mathcal{F}[f(\tau)] = &\int_{-\infty}^{0} \frac{\frac{d}{d\tau}\left\{\exp\left[-P\left(-q_1\tau+\sum_{i=2}^{n}\frac{q_i}{\eta_i}(e^{\eta_i\tau}-1)\right)-j\omega\tau\right]\right\}}{\left[-P\left(-q_1+\sum_{i=2}^{n}q_ie^{\eta_i\tau}\right)-j\omega\right]}d\tau \\ &+\int_{0}^{\infty} \frac{\frac{d}{d\tau}\left\{\exp\left[-P\left(q_1\tau+\sum_{i=2}^{n}\frac{q_i}{\eta_i}(e^{-\eta_i\tau}-1)\right)-j\omega\tau\right]\right\}}{\left[-P\left(q_1-\sum_{i=2}^{n}q_ie^{-\eta_i\tau}\right)-j\omega\right]}d\tau \end{aligned}$$

$$\begin{aligned} F(\omega) = -P\Bigg[&\sum_{i=2}^{n} q_i\eta_i\left\{\frac{\exp\left[-P\left(-q_1\tau+\sum\frac{q_i}{\eta_i}(e^{\eta_i\tau}-1)\right)-j\omega\tau+\eta_i\tau\right]}{\left[-P\left(-q_1+\sum q_ie^{\eta_i\tau}\right)-j\omega\right]^2\left[-P\left(-q_1+\sum q_ie^{\eta_i\tau}\right)-j\omega+\eta_i\right]}\right\}_{-\infty}^{0} \\ &-\sum_{i=2}^{n} q_i\eta_i\int_{-\infty}^{0}\exp\left[-P\left(-q_1\tau+\sum\frac{q_i}{\eta_i}(e^{\eta_i\tau}-1)\right)-j\omega\tau+\eta_i\tau\right] \\ &\times\frac{d}{d\tau}\left\{\frac{1}{\left[-P\left(-q_1+\sum q_ie^{\eta_i\tau}\right)-j\omega\right]^2\left[-P\left(-q_1+\sum q_ie^{\eta_i\tau}\right)-j\omega+\eta_i\right]}\right\}d\tau \\ &+\sum_{i=2}^{n} q_i\eta_i\left\{\frac{\exp\left[-P\left(q_1\tau+\sum\frac{q_i}{\eta_i}(e^{-\eta_i\tau}-1)\right)-j\omega\tau-\eta_i\tau\right]}{\left[-P\left(q_1-\sum q_ie^{-\eta_i\tau}\right)-j\omega\right]^2\left[-P\left(q_1-\sum q_ie^{-\eta_i\tau}\right)-j\omega-\eta_i\right]}\right\}_{0}^{\infty} \\ &-\sum_{i=2}^{n} q_i\eta_i\int_{0}^{\infty}\exp\left[-P\left(q_1\tau+\sum\frac{q_i}{\eta_i}(e^{-\eta_i\tau}-1)\right)-j\omega\tau-\eta_i\tau\right] \\ &\times\frac{d}{d\tau}\left\{\frac{1}{\left[-P\left(q_1-\sum q_ie^{-\eta_i\tau}\right)-j\omega\right]^2\left[-P\left(q_1-\sum q_ie^{-\eta_i\tau}\right)-j\omega-\eta_i\right]}\right\}d\tau\Bigg] \end{aligned} \tag{47}$$

For $1/f$ noise we need the following Fourier transform:

$$S'_{1/f} = \mathcal{F}[f(\tau)\cos(\omega_0\tau)] = \frac{1}{2}F(\omega-\omega_0)+\frac{1}{2}F(\omega+\omega_0)$$
$$= \frac{P}{(\omega-\omega_0)^2}\sum_{i=2}^{n}\frac{\eta_i^2 q_i}{\eta_i^2+(\omega-\omega_0)^2} + \frac{P}{(\omega+\omega_0)^2}\sum_{i=2}^{n}\frac{\eta_i^2 q_i}{\eta_i^2+(\omega+\omega_0)^2}.$$

At RF frequencies $(\omega+\omega_0)^2$ becomes very large and hence the second term becomes quite small compared to the first and can be neglected in a ssb representation

$$S'_{1/f,\mathrm{ssb}}(\omega) \approx \frac{P}{(\omega-\omega_0)^2}\sum_{i=2}^{n}\frac{\eta_i^2 q_i}{\eta_i^2+(\omega-\omega_0)^2} \quad (\omega>0\,\text{only.})$$

ACKNOWLEDGMENT

The authors are grateful to the reviewers for their useful comments which greatly improved the paper. The authors would like to thank Mr. Wetterskog of Texas Instruments for coordination of the TI Graduate Student Fellowship. The second author would like to thank Prof. Obregon and Prof. Nallatamby of IRCOM for valuable and fruitful technical discussions.

REFERENCES

[1] J. Roychowdhury, A. Demir, and A. Mehrotra, "Phase noise in oscillators: A unifying theory and numerical methods for characterization," *IEEE Trans. Circuits Syst. I, Fundam. Theory Appl.*, vol. 47, no. 5, pp. 655–674, May 2000.

[2] D. B. Leeson, "A simple model of feedback oscillator noise spectrum," *Proc. IEEE*, vol. 54, no. 2, pp. 329–330, Feb. 1966.

[3] B. Razavi, "Analysis, modeling and simulation of phase noise in monolithic voltage-controlled oscillators," in *Proc. IEEE Custom Integr. Circuit Conf.*, May 1995, pp. 323–326.

[4] A. Hajimiri and T. H. Lee, "A general theory of phase noise in electrical oscillators," *IEEE J. Solid-State Circuits*, vol. 33, no. 2, pp. 179–194, Feb. 1998.

[5] E. Hafner, "The effect of noise in oscillators," *Proc. IEEE*, vol. 54, no. 2, p. 179, Feb. 1937.

[6] F. X. Kaertner, "Analysis of White and $f^{-\alpha}$ noise in oscillators," *Int. J. Circuit Theory Appl.*, vol. 18, pp. 485–519, 1990.

[7] J. C. Nallatamby, R. Sommet, M. Prigent, and J. Obregon, "Semiconductor device and noise sources modeling, Design method and tools, oriented to nonlinear H.F. oscillator CAD," in *Proc. SPIE*, 2004, vol. 5470, pp. 373–389.

[8] K. Kurokawa, *Microwave Solid State Oscillator Circuits*, 2nd ed. Reading, MA: Addison-Wesley, 1968.

[9] H.-J. Thaler, G. Ulrich, and G. Weidmann, "Noise in IMPATT diode amplifiers and oscillators," *IEEE Trans. Microw. Theory Tech.*, vol. MTT-19, no. 8, Aug. 1971.

[10] A. Demir, "Phase noise and timing jitter in oscillators with colored-noise sources," *IEEE Trans. Circuits Syst. I, Fundam. Theory Appl.*, vol. 49, no. 12, pp. 1782–1791, Dec. 2002.

[11] B. N. Limketkai, "Oscillator modelling and phase noise," Ph.D. dissertation, Elect. Eng. Comp. Sci. Dept., Univ. California , Berkeley, 2004.

[12] E. S. Ferre-Pikal *et al.*, "Draft revision of IEEE STD 1139-1988 standard definitions of physical quantities for fundamental frequency theory and applications," in *Proc. IEEE Int. Freq. Contr. Symp.*, May 28–30, 1997, pp. 338–357.

[13] H. Risken, *The Fokker-Planck Equation*, 2nd ed. New York: Springer-Verlag, 1989.

[14] T. H. Lee, *The Design of CMOS Radio Frequency Integrated Circuits*. Cambridge, U.K.: Cambridge University Press, 1998.

[15] W. A. Edson, "Noise in oscillators," *Proc. IRE*, pp. 1454–1466, 1960.

[16] A. Hajimiri and T. H. Lee, "Design issues in CMOS differential *LC* oscillators," *IEEE J. Solid-State Circuits*, vol. 34, no. 5, pp. 717–724, May 1999.

[17] A. Van Der Ziel, *Noise Sources, Characterization, Measurement*, 1st ed. Englewood Cliffs, NJ: Prentice-Hall, Inc., 1970.

[18] A. Papoulis, *Probability, Random Variables, and Stochastic Processes*, 2nd ed. New York: McGraw Hill, 1984.

[19] G. Gonzalez, *Microwave Transistor Amplifiers*, 2nd ed. Englewood Cliffs, NJ: Prentice-Hall, Inc., 1996.

[20] K. Kurokawa, "Noise in synchronized oscillators," *IEEE Trans. Microw. Theory Tech.*, vol. MTT-16, no. 4, pp. 234–240, Apr. 1968.

Jayanta Mukherjee received the B.Eng. degree from Birla Institute of Technology, Mesra, India, in 1999, and the M.S. and Ph.D. degrees in electrical and computer engineering from the Ohio State University, Columbus, in 2003 and 2006, respectively.

Presently, he is with the Department of Electrical Engineering, Indian Institute of Technology, Mumbai, India, as an Assistant Professor. His research interests include RFIC design, testing, and modeling.

Dr. Mukherjee was awarded the University Gold Medal at Birla Institute of Technology for the highest GPA in his major. From 2001 to 2005, he was a Texas Instruments Fellow.

Patrick Roblin (M'85) was born in Paris, France, in September 1958. He received the Maitrise de Physics degree from the Louis Pasteur University, Strasbourg, France, in 1980, and the M.S. and D.Sc. degrees in electrical engineering from Washington University, St. Louis, MO, in 1982 and 1984, respectively.

In 1984, he joined the Department of Electrical Engineering, at The Ohio State University (OSU), Columbus, as an Assistant Professor and is currently a Professor. His present research interests include the measurement, modeling, design and linearization of nonlinear RF devices and circuits such as oscillators, mixers, and power-amplifiers. He is the first author of a textbook on *High-Speed Heterostructure Devices* (Cambridge University Press, 2002). He is the founder of the Nonlinear RF Research Laboratory at OSU. At OSU, he has developed two educational RF/microwave laboratories and associated curriculum for training both undergraduate and graduate students.

Siraj Akhtar (M'05) received the B.S. degree in electrical engineering (*summa cum laude*) from the University of Mississippi, Mississippi, in 1993, and the M.S. and Ph.D. degrees , in electrical engineering, from the Ohio State University in 1996 and 2000, respectively.

He was a NEC/Litton Fellow, A Lucent Fellow, and a Teaching and Research Associate while at Ohio State. He is currently a RF IC Design Manager in the Radio Design Organization, Wireless Terminal Business Unit, Texas Instruments, Dallas. His interests are in the RF and analog circuit implementation of cellular transmitters in deep-submicrometer CMOS.

Dr. Akhtar was a recipient of the Taylor Medal—the highest academic achievement award conferred by the university, while at the University of Mississippi. He is a member of Eta Kappa Nu, Tau Beta Pi, and Phi Kappa Phi.